# The milliarcsecond scale structure of low frequency variable sources

J. Romney<sup>1</sup>, L. Padrielli<sup>2</sup>, N. Bartel<sup>1,3</sup>, K.W. Weiler<sup>1,4</sup>, A. Ficarra<sup>2</sup>, F. Mantovani<sup>2</sup>, L.B. Bââth<sup>5</sup>, L. Kogan<sup>6</sup>, L. Matveenko<sup>6</sup>, I.G. Moiseev<sup>7</sup>, and G. Nicholson<sup>8</sup>

- <sup>1</sup> Max-Planck-Institut für Radioastronomie, Auf dem Hügel 69, D-5300 Bonn 1, Federal Republic of Germany
- <sup>2</sup> Istituto di Radioastronomia, Via Irnerio 46, I-40126 Bologna, Italy
- <sup>3</sup> Harvard-Smithsonian Center for Astrophysics, 60 Garden St., Cambridge, MA 02138, USA
- <sup>4</sup> Division of Astronomical Sciences, National Science Foundation, Washington, DC 20550, USA
- <sup>5</sup> Onsala Space Observatory, S-43900 Onsala, Sweden
- <sup>6</sup> Institute for Space Research, Academy of Sciences, Moscow, USSR
- <sup>7</sup> Crimea Astrophysical Observatory, Academy of Sciences, Moscow, USSR
- <sup>8</sup> National Institute for Telecommunications Research, Johannesburg, South Africa

Received November 24, 1983; accepted January 9, 1984

Summary. As part of a program of studying compact radio sources which show variability in their radio flux density at low frequencies ( $<1\,\mathrm{GHz}$ ), we have undertaken to map the VLBI structure of 21 such objects. Using a rough "cross antenna" extending from Crimea, USSR in the east to Owens Valley, California in the west and from Onsala, Sweden in the north to Hartebeesthoek, South Africa in the south at 1.7 GHz, it was possible to obtain maps with a resolution of  $\sim 3$  milliarcsec for all sources. Most of these maps are new, the sources never having been mapped with VLBI techniques previously.

As a confirmation of the expectation that low frequency variable sources are generally compact, *all* of the objects were detected in the observations and showed structures on milliarcsecond scales. By roughly grouping the objects into known morphologies, 48% could be classified as asymmetric ("core-jet") structures, 10% had extended, symmetric structures, 14% had "simple" slightly resolved or unresolved structures, and 28% showed more complex structures. The present work represents the initial epoch and therefore does not concentrate on model comparisons or interpretation. However, new VLBI observations are being made and 408 MHz total intensity monitoring is continuing so that a more detailed comparison of theoretical models with observational results can be performed in future papers.

**Key words:** low frequency variables – interferometry – VLBI – radio sources: general

#### I. Introduction

Since the first widely-accepted detections of variability in the mid-1960's (see e.g. a review by Kellermann and Pauliny-Toth, 1968), many extragalactic sources have been found to show large flux density changes on time scales of months to years at frequencies above 1 GHz. These variations seem to be caused by outbursts in the compact nuclei of objects such as quasars, BL Lacertae objects and "active galaxies" and are presumed to bear directly on the

Send offprint requests to: K. W. Weiler (Washington address)

theories for the creation, development and maintenance of radio sources. A number of models have been used to try to explain the phenomenon and while these fit the observations of some sources at centimeter wavelengths reasonably well, they generally predict a decrease in amplitudes of variation with decreasing frequency to the extent that no variation should be observable below about 1 GHz.

However, Hunstead (1972) and later other authors (Stannard et al., 1975; Cotton, 1976a, b; McAdam, 1976; Stannard and Bentley, 1977; Fanti et al., 1979, 1981) have reported large variations in intensity for extragalactic radio sources at decimeter wavelengths. Although attempts have been made to theoretically explain this Low Frequency Variability (LFV) (Cocke and Pacholczyk, 1975; Jones and Burbidge, 1973), no completely satisfactory description seems to exist at present.

For an incoherent synchrotron source, the "self" inverse Compton process implies a minimum size of

$$\theta_{ic}(arcsec) = 1.3 \left\{ \frac{S(v)^{1/2}}{v} \right\} (1+z)^{1/2},$$

where S(v) is the source flux density in Jy, v is the observing frequency in MHz, and z is the source redshift (Fanti et al., 1979). For source components smaller than this, the inverse Compton process should cause very high optical and X-ray fluxes (much higher than observed) and the lifetimes of the relativistic electrons should be too short to fill the whole source volume. On the other hand, for a variable source the so-called "causality argument," i.e., that the variability time scale must be longer than the light travel time across the source, implies a maximum source size of

$$D \sim c\tau$$
,

where D is the linear source diameter, c is the speed of light, and  $\tau$  is the time scale of the variation.

For variable sources observed at centimeter wavelengths, these two size scales are rarely in disagreement. They do conflict, however, for variations at low frequencies where the minimum inverse Compton sizes are much larger. There, the short variability time scales observed for some sources imply *maximum* "causality" sizes on the order of several tens of microarcseconds which are much smaller than the *minimum* inverse Compton sizes, usually on the order of several milliarcseconds (Fanti et al., 1979, 1983). For

**Table 1.** System parameters

Station	$T_{ m system} \ ( m K)$	Sensitivity (Jy K <sup>-1</sup> )		
Crimea, USSR	120	16		
Effelsberg, West Germany	70	1.5		
Fort Davis, Texas	125	10		
Green Bank, West Virginia	70	3		
Hartebeesthoek, South Africa	145	17		
Onsala, Sweden	25	10		
Owens Valley, California	100	6		

this reason, low frequency variability has often been called "Superluminal Flux Variation." Several models such as anisotropic electron motions, relativistically expanding sources, and non-cosmological redshifts have been suggested to explain this phenomenon.

As a part of our more general study of LFV, we have undertaken Very Long Baseline Interferometry (VLBI) measurements to determine the apparent sizes, structures, and brightness temperatures in these low frequency variable sources. The present observations provide us with first epoch information for the study of source structure changes with time and with flux density variations.

### II. Observations and data analysis

The observations were made at 1.667 GHz (18 cm wavelength) in left-hand circular polarization during 48 hours on 14–16 February 1980 using a cross-type VLBI array with 7 telescopes. The telescopes are listed in Table 1 along with their system temperatures and sensitivities. The observing frequency was chosen as a compromise between a low frequency, at which the superluminal flux density variations have been observed but at which VLBI resolution is low and the interstellar scattering is high, and a high frequency, at which the variable components of interest may not be observed but at which the resolution is high and the interstellar scattering is low. At 1.7 GHz the resolution of our interferometer is high enough,  $\sim 3$  milliarcsec (mas), that it should be possible to see source structure changes on the time scales of low frequency variations.

The sources observed in the program consist of objects found to be variable or possibly variable at 0.4 GHz in the monitoring program of Fanti et al. (1979). Additionally, several sources which were found to be variable or possibly variable at 0.4 GHz in a subsequent part of the monitoring program (Fanti et al., 1981) were added to the program.

The basic properties of the sources in the program are given in Table 2. The first column lists the IAU designation for the source while the second and third columns give the right ascension and declination of the field center for which the data were correlated.

Table 2. Source properties

IAU	Position <sup>1</sup>		Integrated Flux Density	Variability Index at 0.4 GHz <sup>3</sup>	Optical Ident.	Optical 4 Magnitude	Red-4 Shift	Spectral Index at 0.4 GHz <sup>5</sup>	Spectral Type	F <sub>x</sub> (Ref.) (0.5-4.5keV)	Other Names
	RA (1950) hms	Dec (1950)	S <sub>1</sub> (Z <sub>y</sub> )Hz	ΔS/\$ (%)		m	z			10 <sup>-12</sup> erg cm <sup>-2</sup> s <sup>-1</sup>	
0202+149	020207.403	+145950.95	3.9	10 (V)	QSS	-	-	0.0	FC-	<0.6(6)	NRAO 091, 4C15.05
0224+671	022441.175	+670739.70	1.4	18 (V)	QSS	19.5	-	0.0	FC-		4C67.05
0316+413	031629.560	+411951.89	20.5	1 (P)	GAL	12.5	0.018	1.0	SC+	95(7)	3C84, NGC1275
0333+321	033322.400	+320836.67	3.0	19 (V)	QSS	17.5	1.253	0.0	FS	4(8)	NRAO 140
0405-123	040527.5 <sup>2</sup>	<b>-</b> 121932.3 <sup>2</sup>	2.9	<5 (N)	QSS	16.0	0.574	0.7	SS	5.1(7)	
0422+004	042212.52	+002916.65	1.0	14 (P)	QSS	17.0	-	0.1	FS	1.8(6)	
0605-085	060536.027	-083420.30	2.5	12 (V)	QSS	18.0	-	0.3	FC+		OH-010
0607-157	060726.00	-154203.1	1.5	33 (V)	QSS	17.0	0.324 <sup>5</sup>	0.0	FS		
0723-008	072317.837	-004855.40	2.3	22 (V)	QSS	18.0	0.128	0.0	FS	1.1(6)	
0736+017	073642.513	+014400.20	2.7	23 (V)	QSS	18.0	0.191	0.0	FS	2.6(6)	
0859-140	085954.95	-140338.85	2.7	18 (V)	QSS	18.0	1.327	0.3	FS	1.2(7)	OJ-199
1055+018	105555.316	+015003.45	2.9	12 (V)	QSS	18.0	0.888	0.1	FS		4C01.28
1116+128	111620.777	+125106.65	2.0	<6 (N)	QSS	19.0	2.118	0.3	FS		4C12.39
1127-145	112735.673	-143254.4	6.2	12 (V)	QSS	17.0	1.187	-0.1	FS		OM-146
1504-166	150416.419	-164059.25	^2	23 (V)	QSS	18.5 <sup>5</sup>	0.876 <sup>5</sup>	0.2	FS	2.5(9)	OR-102
1510-089	151008.903	-085447.55	2.7	31 (V)	QSS	18.0	0.361	0.0	FS	<0.4(7)	OR-017
1611+343	161147.916	+342019.82	2.1	29 (V)	QSS	17.5	1.404	0.1	FS		DA 406
1641+399	164117.608	+395410.82	7.5	11 (V)	QSS	16.5	0.594	0.2	FC+	4.4(10)	30345, 4039.48
1730-130	173013.534	-130245.78	5.7	5 (P)	QSS	19.0	0.900	0.2	FC-	1(8)	NRAO 530
2200+420	220039.359	+420208.57	1.9	37 (V)	BL	14.0	0.07	-0.3	F	3.6(7)	BL LAC, VRO42.22.01
2251+158	225129.521	+155254.31	10.1	26 (V)	QSS	18.0	0.859	0.0	FC+	3.1(10)	30454.3, 4015.76

<sup>5</sup>Fanti <u>et al.</u> (1983)

Perley, 1982 2Nominal position used for fringe stopping 3Fanti et al, (1981) 2Veron and Veron (1974, 1978 update)

Gowen et al. (1981)
Junpublished results (LP & NB)
Marscher and Broderick (1981)
Ku et al. (1980)
Tananbaum et al. (1983)

Column 4 gives the 1.7 GHz integrated flux densities of the sources at the time of the VLBI observations. These were determined from the total power records on the Effelsberg 100 m telescope to an accuracy of  $\sim 10\%$ . Column 5 gives the Variability Index of each source at 0.4 GHz from the work of Fanti et al. (1981). The Variability Index or fractional variability is defined by Fanti et al. as  $\Delta S/\overline{S}$  expressed in percent (%) where  $\overline{S}$  is the weighted average flux density of the source over the entire sample of their 0.4 GHz observations and  $\Delta S$  is defined as

$$\Delta S = 3[(rms)^2 - \bar{\sigma}_e^2]^{1/2}$$

where rms is the root mean square deviation of the source flux density measurements and  $\bar{\sigma}_e$  is the expected error for the measurements. The determination of  $\bar{\sigma}_e$  is discussed in more detail in the Fanti et al. (1981) work. Also included in column 5 is an indication of whether the source was found to be variable (V), probably variable (P) or not variable (N) in the 0.4 GHz monitoring. In fact, two of the objects (0405-123 and 1116+128) included in the observations do not show significant variability in the longer series of measurements.

Columns 6–8 list the optical identification, approximate optical magnitude, and redshift, respectively. These values are taken from the work of Véron and Véron (1974) except where otherwise noted. The identifications are noted as quasi-stellar source (QSS), galaxy (GAL), or BL Lacertae-type object (BL).

Column 9 gives the radio spectral index  $(S \propto v^{-\alpha})$  near 0.4 GHz from Fanti et al. (1983). Column 10 notes the radio spectral morphology near 0.4 GHz (Fanti et al., 1983). The first letter designation, F or S (flat or steep spectrum), denotes a spectral index  $\alpha$  near 0.4 GHz of  $\alpha \le 0.4$  or  $\alpha > 0.4$ , respectively. The second letter and sign designation, S or  $C \pm$ , denote spectra which are straight over a large frequency range (S) or which either steepen (C-) or flatten (C+) significantly at higher frequencies. A full description of the spectral classification and a discussion of the relation between low frequency variability and spectral class can be found in Fanti et al. (1983). It is apparent that the sources with a flat radio spectrum over a very large range of frequencies have the highest probability of showing LFV.

In column 11 is listed the X-ray flux density. The enormous difference between these detected X-ray flux densities and those expected from the inverse Compton effect, if the extremely high brightness temperatures implied by rapid low frequency variability were true, is discussed further by Fanti et al. (1983).

In the last column (column 12) other common names for the sources are given.

With careful planning of the observations, it was possible to observe each source about 10 times during the 48-h period with occasional split scheduling of the eastern and western sub-arrays to maximize the efficiency of the program. Of the 21 available baselines in the array, 17 were correlated, all of which yielded useful data. Typically, visibility measurements were obtained at 40 to 50 different locations in the observation (U-V) plane with 2 or 3 independent coherent integrations at each location.

Correlation of the data was carried out on the Mark II, 3-station correlator of the Max-Planck-Institut für Radioastronomie in Bonn, Germany. The stability of the interferometers was sufficient to permit coherent integrations of the data over an interval of 225 s with a reduction of the signal intensity of <5%. The four sources used to calibrate the data (0440-003, 0851+202, 1404+286,and 2345-168),along with their assumed simple elliptical gaussian structure models, are described by Matveenko et al. (1981). Calibration of the correlation coefficients resulted in a b-factor of  $\sim 2.6$  with a set of

second-order corrections ( $\sim \pm 0.2$ ) for each station (see, e.g., Cohen et al., 1975). On some of the baselines without crossing points in the U-V plane, correction coefficients were obtained by considering the systematic differences of fringe visibility plots between the simple models and the actual data for the calibration sources. These additional corrections were <12% for each station with an uncertainty of <  $\pm 4\%$ .

Among the 29 sources which were observed (25 unknowns and 4 calibrators), two [0632+191 and 1358+624 (4C62.23)] were later found to have had such poor field center positions that they did not produce usable data. Also, 1524-136 (OR-140) and 1416+066 (3C298) apparently had such complicated structures that it was not possible to map them by this "snapshot" technique.

In order to try to eliminate personal biases, the calibrated data were analyzed independently at three institutions, Bologna, Bonn, and MIT. Also, the Soviet participants independently analyzed 0316+413 (3C84) and 1641+399 (3C345) (Matveenko et al., 1981, 1982). Maps were obtained through "hybrid mapping" techniques adapted from the methods of Cornwell and Wilkinson (1981) (Bologna and Bonn) and through the similar methods of Readhead and Wilkinson (1978) (MIT). The "CLEAN" procedure was always deep enough to reduce the residual map below 2% of the peak source brightness.

The "restoring beam" used in all cases was an elliptical gaussian fitting the inner part of the "dirty" beam. When the principal source structure was in the north-south (N/S) direction and the "dirty" beam had several side-lobes higher than 50% (see, e.g., Figs. 1c and 1d), a map was also obtained with a restoring beam whose N/S gaussian diameter corresponded to the outermost 50% contour of the "dirty" beam. This last is roughly the beam which would have been obtained without the South African station in the network. Examples of "dirty" beams at different declinations are given in Fig. 1.

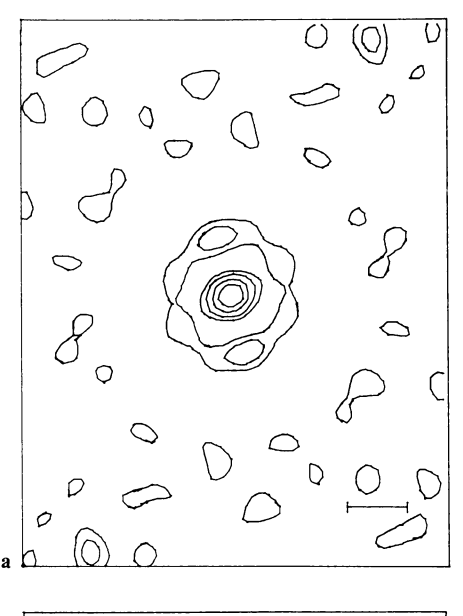
A comparison showed good agreement among the several solutions for most sources. In cases where significant differences occurred, the solution providing the best fit to the amplitude and phase closure data was chosen. In all but a few cases (commented on separately for the individual sources) the correspondence between the fringe visibilities and phase closure data was quite good ( $<1\sigma$ ).

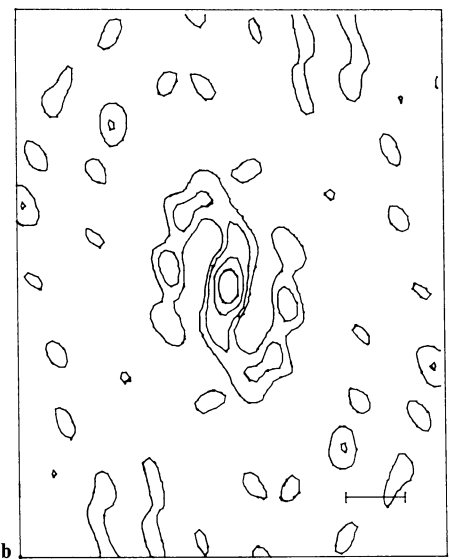
The reliability of the source maps is considered to be high. Each "hybrid mapping" procedure was initiated with an approximate, multi-component gaussian model for the source with the fitting procedure then iterating until the solution did not change significantly after 2 or 3 additional cycles. The fit of the Fourier transform of the resulting source map to the original data and its closure phases was then examined and considered to be acceptable when the differences did not exceed  $1\sigma$  with  $1\sigma$  defined as the rms noise in the map plus a 5% calibration error. All contour levels shown for the final maps presented below are considered to be significant.

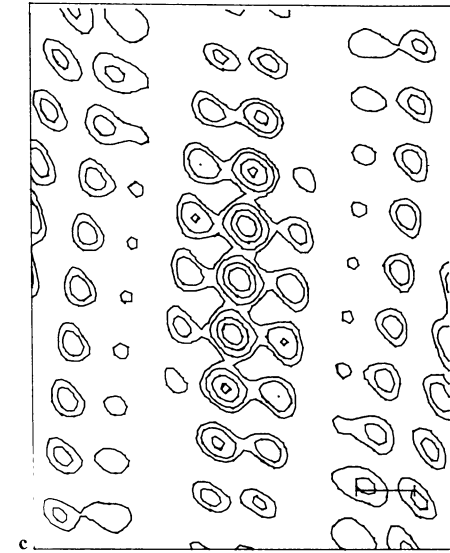
## III. Results and discussion

Table 3 lists the major characteristics of the maps. The first column gives the IAU designation, the second gives the total flux density in the VLBI map and the third column gives the peak source brightness in Jy/beam area (Jy ba $^{-1}$ ). The error in this last value is estimated to be  $\sim 5$ –10%. It can be converted to a brightness temperature through the relation

 $T_b(K) \approx 5 \cdot 10^{11} B_{\text{peak}}(\text{Jy ba}^{-1}) \theta_{\text{max}}^{-1}(\text{mas}) \theta_{\text{min}}^{-1}(\text{mas}),$ 







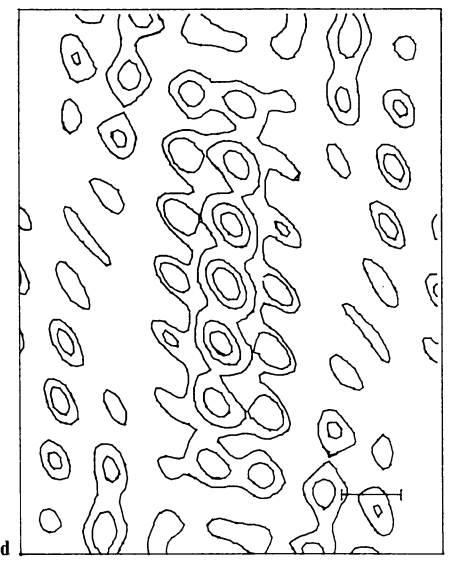


Fig. 1a-d. Examples of "dirty" beams for 4 typical sources at different declinations: a 0224+671 ( $+67^{\circ}$ ), b 0333+321 ( $+32^{\circ}$ ), c 1055+018 ( $+2^{\circ}$ ), d 1504-166 ( $-17^{\circ}$ ). The contours are  $10^{\circ}$ 0, 25%, 50%, 75%

where  $T_b$  is the source peak brightness temperature in degrees Kelvin,  $B_{peak}$  is the measured peak brightness in Janskys per beam area and  $\hat{\theta}_{max}$  and  $\theta_{min}$  are the major and minor axes, respectively, of the restoring beam in milliarcseconds. Column 4 gives the parameters of the restoring gaussian beam as the Full Width at Half Maximum (FWHM) of the major and minor axes in milliarcseconds (mas) and the position angle (p.a.) of the major axis in degrees. The position angle is measured positive from north through east. Column 5 lists the largest angular size of the source structure to the 10% contour in mas and its position angle in degrees. To determine this value in a systematic manner, all sources were restored with a 3 mas FWHM circular beam for the measurement. Columns 6 and 7 give the apparent morphologies of the sources on milliarcsecond scales (VLBI morphology) and arcsecond scales (VLA morphology). A more detailed discussion of the observed properties of the individual sources is given below.

0202+149 (NRAO 091, 4C15.05; Fig. 2a)

The source is slightly extended along a position angle of  $114^{\circ}$ . Since only  $\sim 60\%$  of the source integrated flux density is

accounted for in the map, a larger and completely resolved component of ~1 Jy must be present. However, on the arcsecond size scale the source is unresolved both in 1.4 GHz VLA observations (Perley, 1982) and in a MERLIN map at 0.4 GHz (Mantovani et al., 1984).

0224+671 (4C67.05; Fig. 2b)

The structure consists of a compact core with a weak extension 5 mas long in p.a.  $2^{\circ}$ . The extension aligns very well with a diffuse, weak component  $\sim 10''$  to the north seen in a VLA map (Perley et al., 1982). The VLA map at 1.4 GHz also shows another resolved component  $\sim 7''$  to the south of the core.

0316+413 (3C84, NGC1275; Fig. 2c)

3C84 is a very complicated radio source having structure on scale sizes ranging from milliarcseconds (Unwin et al., 1982) to arcminutes (Miley and Perola, 1975). It is an unusual object in our sample of low frequency variables. 3C84 is the only source having very large angular scale, extended radio structure; it is the only

J. Romney et al.: Low frequency variable sources

**Table 3.** Source map descriptions

IAU Name	VLBI Map Flux Density (Jy)	Bpeak Brightness (Jy/beam area)	Restoring Beam Parameters Major, Minor, p.a. (mas, mas, deg)	Source Largest Angular Size Length, p.a. (mas, deg)	VLBI Morphology (millarcsecond structure)	VLA <sup>1,2</sup> Morphology (arcsecond structure)
0202+149	2.3	0.9	2.5, 18, -5	4, 114	ES	S
02024+671	1.4	0.8	3.5, 2.5, -81	5, 2	EA	T
0316+413	16.2	5.9	3.0, 5.0, -5	7, 174	EA	CPX
0333+321	2.9	1.1	3.0, 6.5, -11	8, 132	ES	D2
0405-123	1.2	0.6	2.5, 4.0, 25	10, 17	S	טב
0403=123	1.2	0.7	2.5, 4.0, 32	<6	S	S
0605-085	2.8	1.2	3.0, 4.5, 19		EA .	D2
0607-157	1.5	0.5	3.0, 4.5, 19	15, 143		
	-		- , ,	20, 38	EA	S
0723-008	2.3	0.6	3.0, 3.5, 39	20,-24	CPX	S
		1.3	3.0, 18, -10			
0736+017	2.9	1.1	3.0, 3.5, 36	13, 72	CPX	S
0859-140	2.6	0.8	3.0, 3.5, 48	26 <b>,-</b> 5	EA	T
		1.6	4.0, 20, <b>-</b> 7			
1055+018	2.7	0.8	2.5, 3.0, 69	10,-56	CPX	D2
1116+128	1.5	0.4	2.5, 3.0, 26	17, 27	EA	D2
		0.7	3.0, 18, <b>-</b> 9			
1127-145	6.0	2.2	2.5, 3.5, 32	9, 18	CPX	S
1504-166	2.0	1.1	2.5, 4.0, 43	6, 146	EA	S
1510-089	2.6	1.9	2.5, 3.0, 26	4, 173	EA	CJ
1611+343	2.5	1.6	2.5, 5.0,-13	<5	S	S
1641+399	6.4	2.9	2.5, 3.5, 14	6,-68	EA	CJ
1730-130	5.7	1.7	2.5, 4.5, 12	26,-7	CPX	D2
<del>-</del>	•	3.0	3.5, 19, -8	,		
2200+420	1.7	0.9	2.5, 3.5, 5	5, 170	EA	S
2251+158	9.6	2.8	3.0, 4.0, 0	12,-60	CPX	CJ

Morphology:

= Simple-compact or slightly resolved

EA = Extended, asymmetric ES = Extended, symmetric

= Triple

D2 = Core and second unattached component

CJ = Core-jet

galaxy in our sample; and it is one of the few very active sources having extremely compact structure which is known to clearly show motions at non-relativistic speeds. The structure seen in Fig. 2c has a north-south alignment, as does much of the larger scale structure in the source (see, e.g., Pauliny-Toth et al., 1976; Miley and Perola, 1975), and has a morphology characteristic of many relativistically beaming sources. Thus, monitoring of any changes in structure of the source will be of primary importance since some current theories attribute both low frequency variability and superluminal motion to the same directed, relativistic beams.

# 0333+321 (NRAO 140; Fig. 2d)

Marsher and Broderick (1982), on the basis of three epoch VLBI observations at 10.7 GHz, find this source to expand superluminally at a rate of 0.10-0.14 mas yr<sup>-1</sup> along a "jet" extended ~5 mas to the southeast. The present 1.7 GHz map clearly shows a "jet" extending to 8 mas in p.a. 132°. The arcsecond scale maps (Browne et al., 1982; Perley, 1982) show a weak component  $\sim 8''$  to the southeast of a bright, unresolved core that is misaligned relative to the milliarcsecond structure by  $\sim 18^{\circ}$ .

The present observations show slightly extended structure 10 mas in size and containing  $\sim 40\%$  of the source flux density. Since the source is bright, compact, and poorly studied, it is obviously a good candidate for higher frequency, higher resolution observations.

$$0422 + 004$$
 (Fig. 2f)

Perley (1982)

2Perley et al. (1982)

With nearly all of its flux density emanating from an almost unresolved region <6 mas in size, the source is very compact. Again, higher frequency, higher resolution observations are needed to determine its detailed structure. VLA observations show no structure on arcsecond scales (Perley, 1982).

The source appears to have an extended, asymmetric structure somewhat resembling a core-jet. The "core" is quite compact while the "jet" extends 15 mas to the southeast. On a larger scale, VLA observations (Perley, 1982) at 1.4 GHz show a secondary component  $\sim 5''$  to the east of the compact core in p.a.  $\sim 96^{\circ}$ . The misalignment between the milliarcsecond and arcsecond structure is thus  $\sim 45^{\circ}$ .

At arcsecond resolution, VLA maps at 1.4 GHz show that the source is unresolved (Perley, 1982). The VLBI source appears to have an extended, asymmetric structure containing most of the flux density. The "jet" is 20 mas long at a position angle of 38°.

The source is unresolved in VLA observations at 1.4 GHz (Perley, 1982). At VLBI resolution, it appears to have an extended, asymmetric structure with the "jet" extending 20 mas at p.a.  $-24^{\circ}$ . Both full resolution (Fig. 2i1) and smoothed restoring beam (Fig. 2i2) maps are shown.

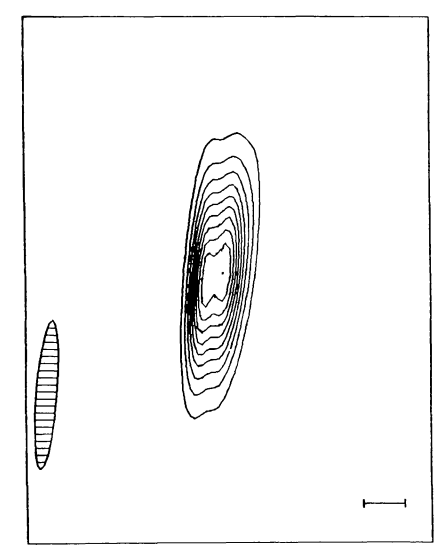
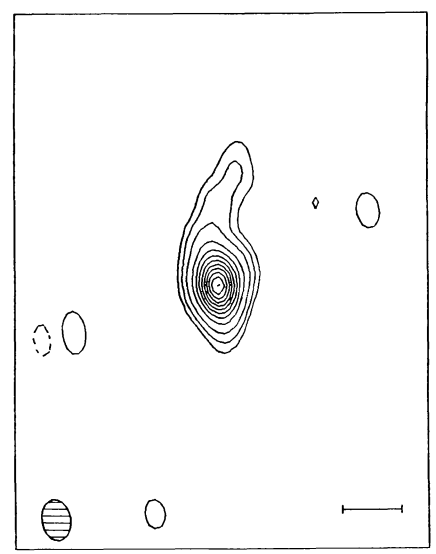


Fig. 2a. Contour map showing the 1.7 GHz milliarcsecond (mas) structure of the low frequency variable source 0202+149 (NRAO 091, 4C15.05). The map is oriented with north at the top and east at the left. The bar in the lower right hand corner is 5 mas in length and the hatched figure in the lower left hand corner illustrates the Full Width at Half Power (FWHP) of the restoring beam. The peak brightness is given in Table 3 and the contour levels, from the peak down, are 100%, 90%...20%, 10%, 5%, 2.5%, -2.5% (dashed). No map contains significant negative contours



**Fig. 2b.** 0224+671 (4C67.05). See the caption to **a** for details

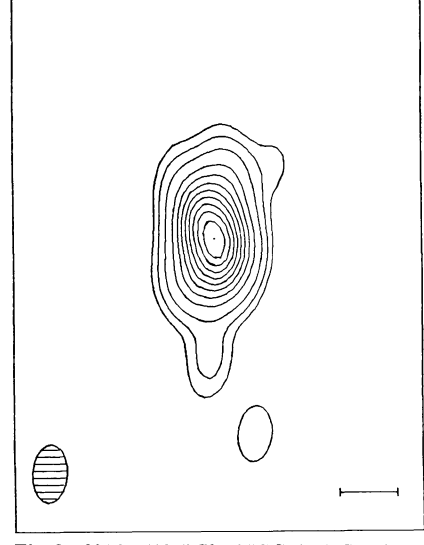


Fig. 2c. 0316+413 (3C84, NGC1275). See the caption to a for details

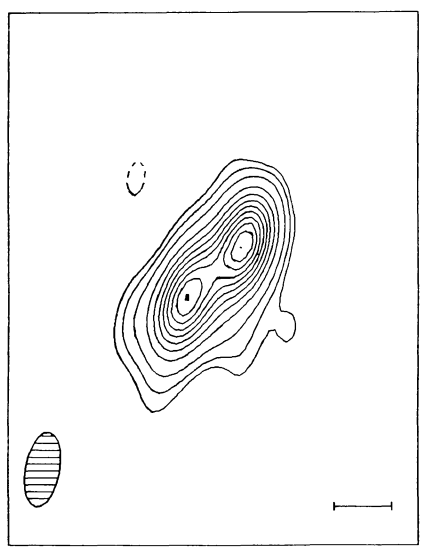


Fig. 2d. 0333 + 321 (NRAO 140). See caption to a for details

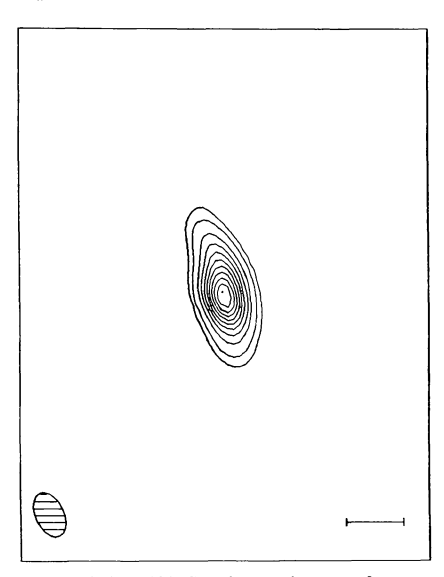
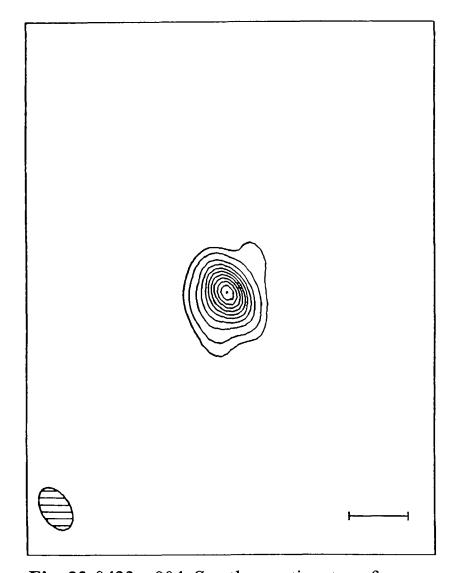


Fig. 2e. 0405-123. See the caption to a for details



**Fig. 2f.** 0422+004. See the caption to **a** for details

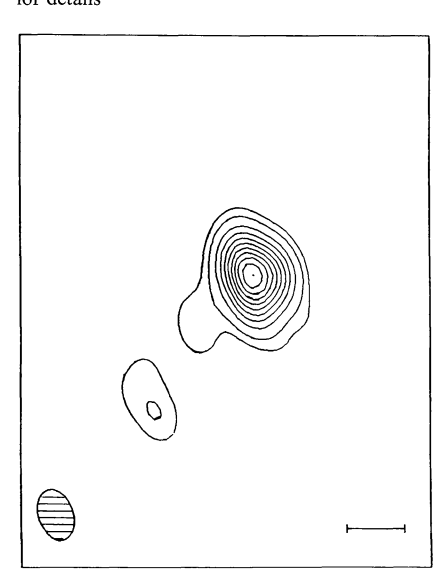
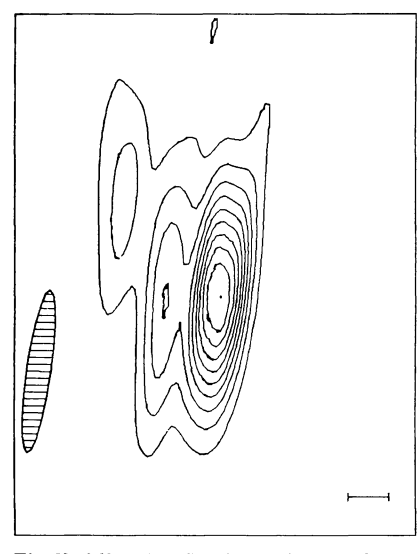


Fig. 2g. 0605-085 (OH-010). See the caption to a for details



**Fig. 2h.** 0607-157. See the caption to **a** for details

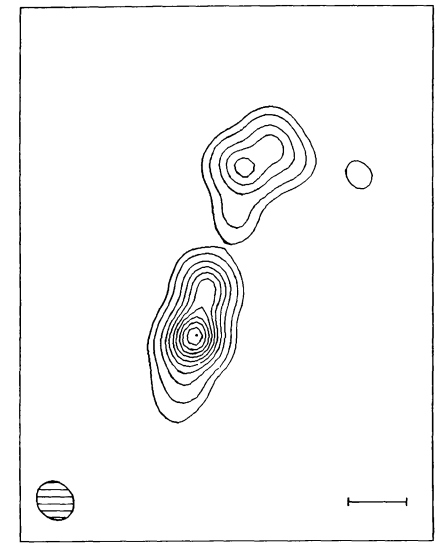


Fig. 2i1. 0723-008 full resolution map. See the caption to **a** for details

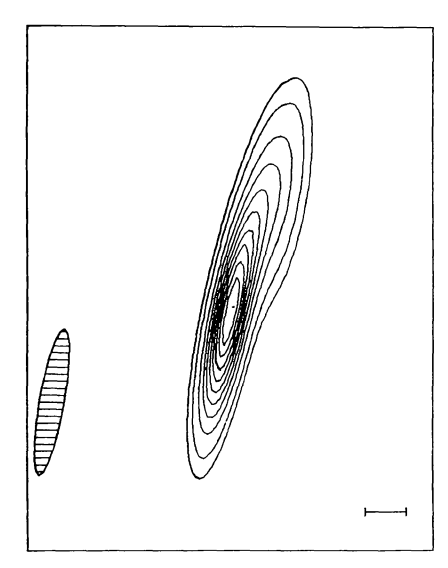


Fig. 2i2. 0723-008 smoothed restoring beam map. See the caption to a for details

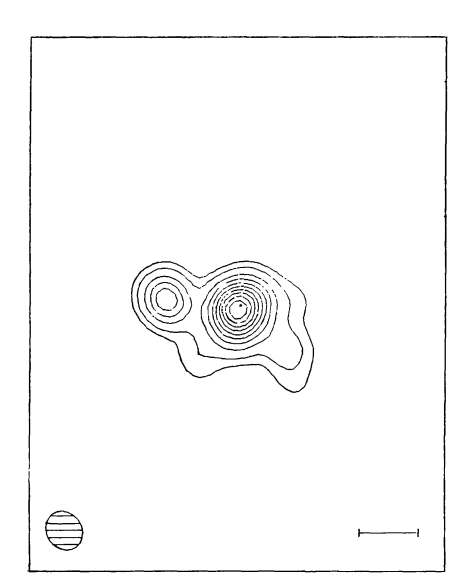


Fig. 2j. 0736 + 017. See the caption to **a** for details

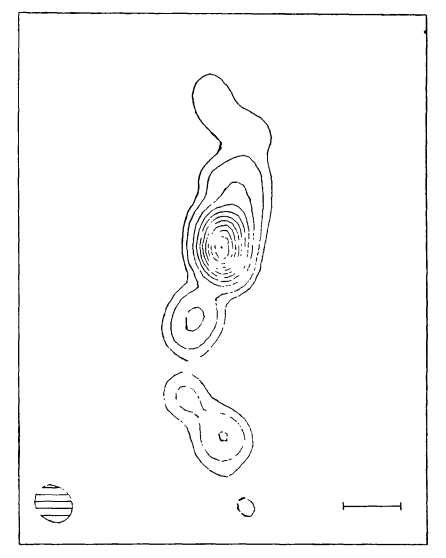


Fig. 2k1. 0859 – 140 (OJ-199) full resolution map. See the caption to a for details

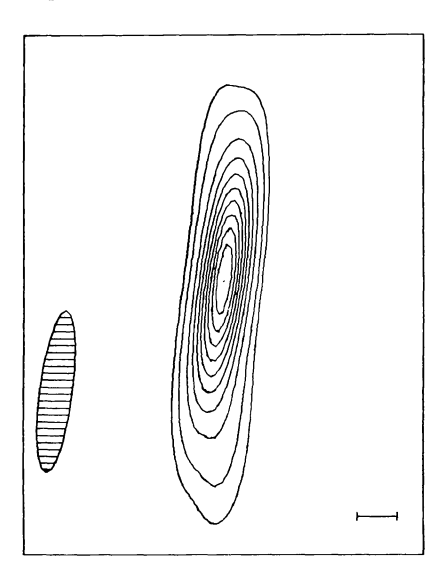
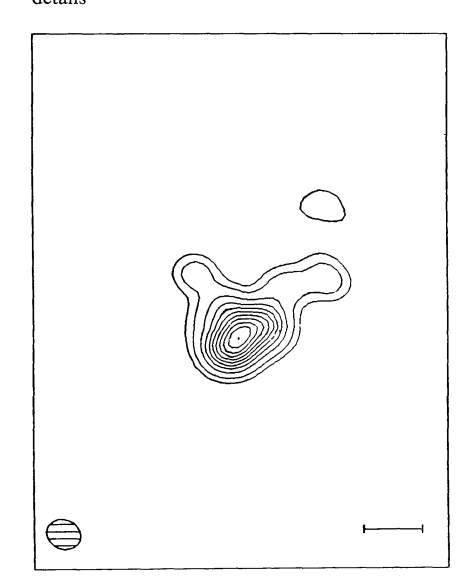


Fig. 2k2. 0859 – 140 (OJ-199) smoothed restoring beam map. See the caption to a for details



**Fig. 21.** 1055+018 (4C01.28). See the caption to **a** for details

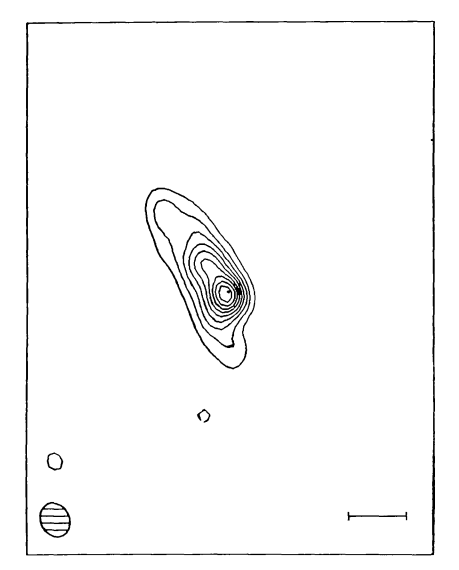


Fig. 2m1. 1116+128 (4C12.39) full resolution map. See the caption to a for details

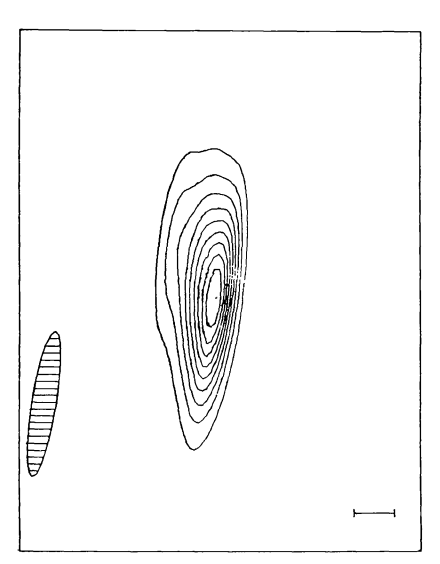
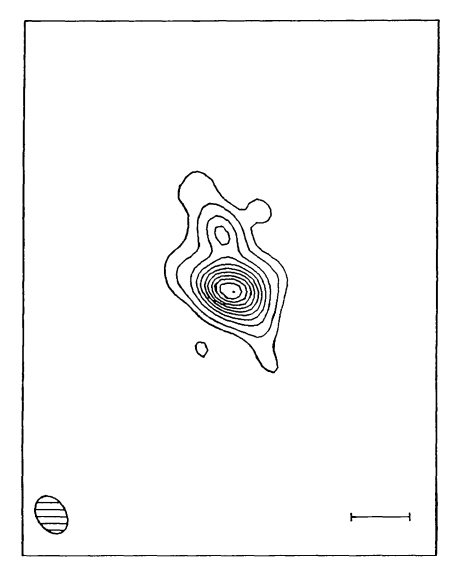
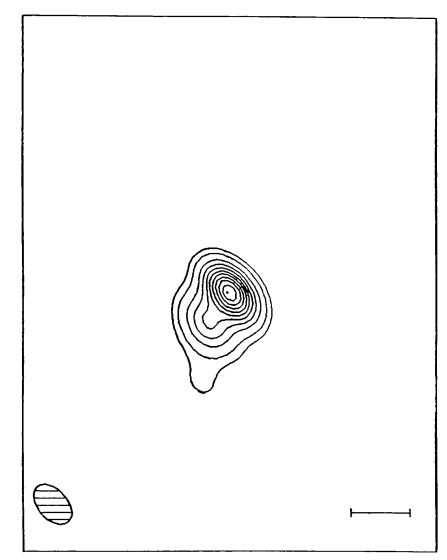


Fig. 2m2. 1116+128 (4C12.39) smoothed restoring beam map. See the caption to a for details



**Fig. 2n.** 1127 – 145 (OM-146). See the caption to **a** for details



**Fig. 20.** 1504 – 166 (OR-102). See the caption to **a** for details

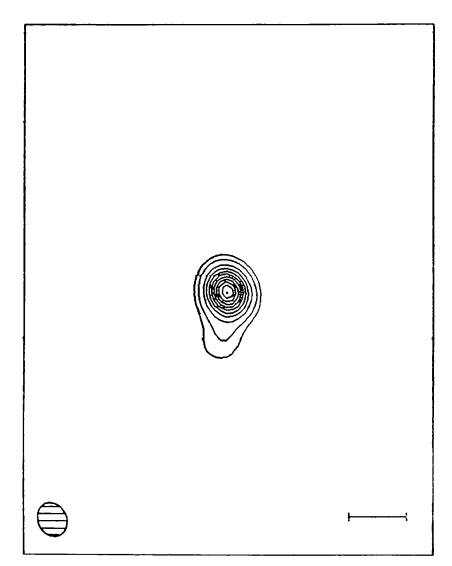


Fig. 2p. 1510-089 (OR-017). See the caption to a for details

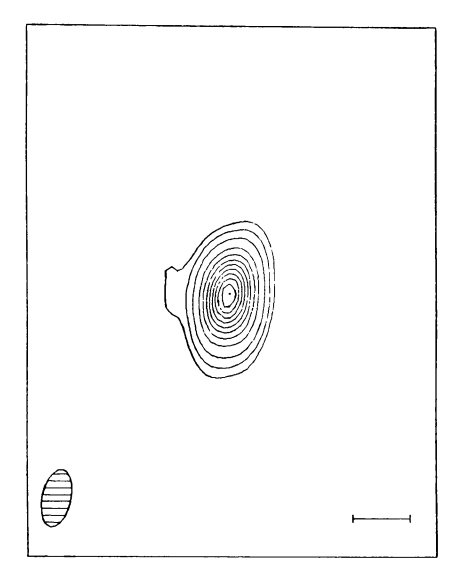


Fig. 2q. 1611 + 343 (DA 406). See the caption to a for details

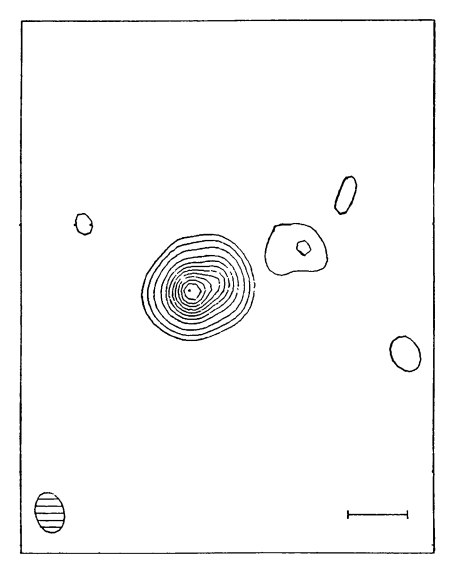


Fig. 2r. 1641 + 399 (3C345, 4C39.48). See the caption to a for details

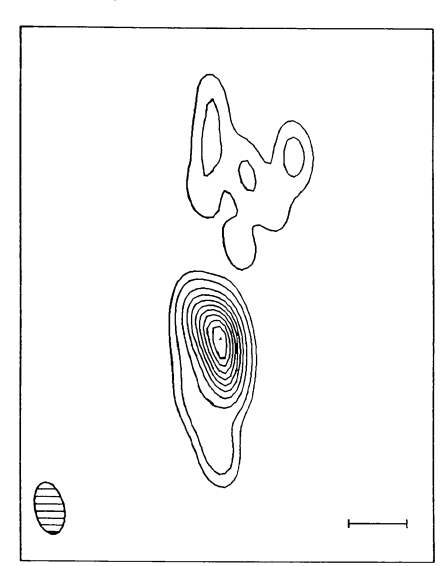


Fig. 2s1. 1730-130 (NRAO 530) full resolution map. See the caption to  $\bf a$  for details

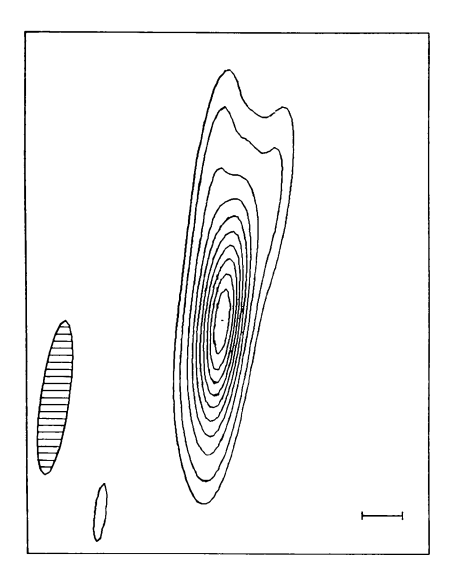


Fig. 2s2. 1730-130 (NRAO 530) smoothed restoring beam map. See the caption to a for details

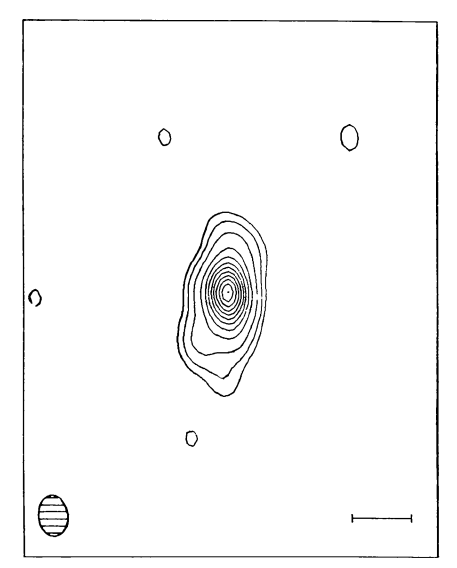
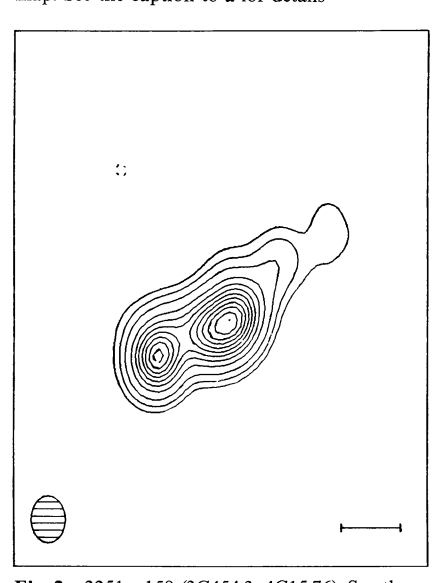


Fig. 2t. 2200+420 (BL Lacertae, VRO 42.22.01). See the caption to a for details



**Fig. 2u.** 2251 + 158 (3C454.3, 4C15.76). See the caption to **a** for details

0736 + 017 (Fig. 2j)

The source shows rough "triple" structure with "lobes" extending on either side of a bright "core." The total size is 13 mas along p.a. 72°. The source is unresolved in VLA observations at 1.4 GHz (Perley, 1982).

0859-140 (OJ-199; Fig. 2k)

This source is one of the most unusual in our sample. Even though it is a strong low frequency variable and contains compact VLBI components, on arcsecond scales it has a classical "triple" morphology of a core source bracketed by extended radio lobes  $\sim 6''$  distant at p.a.  $\sim 10^\circ$ . On the milliarcsecond scale, the source appears extended by 26 mas in p.a.  $-5^\circ$ . Both full resolution (Fig. 2k1) and smoothed restoring beam (Fig. 2k2) maps are shown.

1055+018 (4C01.28; Fig. 2l)

On the arcsecond scale, a VLA map at 1.4 GHz (Perley, 1982) of the source shows a bright, unresolved core with a "jet" extending  $\sim 10''$  at position angle  $\sim 180^\circ$ . On the milliarcsecond scale, the structure appears to have elongations both to the northeast and northwest.

1116+128 (4C12.39; Fig. 2m)

4C12.39 exhibits arcsecond scale structure shown by the VLA at 1.4 GHz to consist of a bright unresolved core and a weaker but compact component  $\sim 2''$  distant in p.a.  $\sim 315^{\circ}$  (Perley, 1982). There is no apparent "bridge" connecting the outer component to the core. On the milliarcsecond scale, the core is elongated with a total size of 17 mas in p.a.  $27^{\circ}$ . Both full resolution (Fig. 2m1) and smoothed restoring beam (Fig. 2m2) maps are shown.

1127-145 (OM-146; Fig. 2n)

The source is slightly extended with an elongation of 9 mas in p.a. 18°. It is unresolved in 1.4 GHz VLA maps (Perley, 1982). For this one source, the phase closure information is insufficient to uniquely determine the source orientation and it is possible that the position angle of the extension could have a 180° error.

1504-166 (OR-102; Fig. 20)

The source is quite compact with a jet-like feature 6 mas long in p.a. 146°. It is unresolved in 1.4 GHz VLA observations (Perley, 1982).

1510-089 (OR-017; Fig. 2p)

On the milliarcsecond scale, the source has a compact core with a jet-like feature 4 mas long at p.a.  $173^{\circ}$ . On arcsecond size scales, a VLA map at 1.4 GHz (Perley, 1982) shows a jet, extending  $\sim 8''$  in length at p.a.  $\sim 160^{\circ}$ .

1611+343 (DA 406; Fig. 2q)

The source is completely unresolved at both arcsecond (Perley, 1982) and milliarcsecond (<5 mas) scales.

1641 + 399 (3C345, 4C39.48; Fig. 2r)

3C345 is one of the most studied and active of the so-called "superluminal" sources. Recent articles (Unwin et al., 1982; Schraml et al., 1981; Cohen et al., 1981) summarize the current status of VLBI monitoring of the rapid structural changes. On

arcsecond scales, a VLA observation at 1.4 GHz (Perley, 1982) shows an unresolved core with a jet  $\sim 2''$  long extending in p.a.  $\sim -30^\circ$ . On milliarcsecond scales, the source shows a slightly resolved core elongated by 5–10 mas at position angle  $-70^\circ$ . This is consistent with other observations showing a compact core <1 mas in size and an extended jet  $\sim 3$  mas long extending at a position angle  $\sim -80^\circ$  (Bååth et al., 1981a, b; Matveyenko et al., 1982). At intermediate scales, MERLIN maps (Browne et al., 1982) show a curving "bridge" of emission connecting the small scale with the large scale structures.

1730-130 (NRAO 530; Fig. 2s)

On arcsecond scales, a VLA map at  $1.4\,\mathrm{GHz}$  of the source (Perley, 1982) shows an unresolved core and a second unresolved, possibly unrelated component  $\sim 11''$  distant in p.a.  $\sim 270^\circ$  with no evidence for a connection between the two sources. The milliarcsecond scale structure is oriented in a north-south direction, extended 26 mas in p.a.  $-7^\circ$ . Both the full resolution (Fig. 2s1) and smoothed restoring beam (Fig. 2s2) maps are shown. The small scale structure is confirmed by the  $10.7\,\mathrm{GHz}$  VLBI observations of Marscher and Broderick (1981).

2200+420 (BL Lacertae, VRO 42.22.01; Fig. 2t)

BL Lac is the defining member of a whole class of sources known as BL Lacertae-type objects or Lacertids. Both the large and small scale structures of the group have recently been discussed by Weiler and Johnston (1980) and Ulvestad et al. (1983). Also Bååth et al. (1981b) have described the milliarcsecond structures of a number of the members of the group including BL Lac itself. The present observations show a very compact source with only slight extension to the south. Recently, Phillips and Mutel (1982) have found the source to expand with an apparent velocity of  $\sim 5c$ .

2251+158 (3C454.3, 4C15.76; Fig. 2u)

This is one of the most strongly varying LFV sources. On the arcsecond scales, a VLA map at 1.4 GHz (Perley, 1982) shows a compact core with a second, compact, weaker component  $\sim\!5''$  distant at position angle  $\sim\!-40^\circ$ . Intermediate resolution MERLIN maps (Browne et al., 1982) show a bridge connecting the core with the outer component. Finally, the present milliarcsecond resolution observations show a structure elongated 12 mas in p.a.  $-60^\circ$ , in good alignment with the outer structure.

#### IV. Conclusions

Twenty-one radio sources chosen on the basis of their known or suspected low frequency ( $<1\,\mathrm{GHz}$ ) variability have been observed for milliarcsecond scale structure. All have been detected by our VLBI interferometer at 1.7 GHz wavelength and all show compact features in their structures. On milliarcsecond scales, the sources show the following:

-10(48%) have asymmetric structures (perhaps one-sided jets) with linear sizes ranging from 2 to 55 pc. ( $H \equiv 100 \text{ km s}^{-1} \text{ Mpc}^{-1}$ .)

- 2(10%) have extended symmetric structures. These two sources, which have only two components, could belong to the previous class if one component were considered to be the core and the other a jet.
- -3(14%) are unresolved or only slightly resolved on a scale of a few mas with physical dimensions <10-30 pc.
- 6(28%) have more complex structures which do not accommodate a simple description.

A comparison between the alignment of arcsecond and milliarcsecond structures in the sources often shows large



298

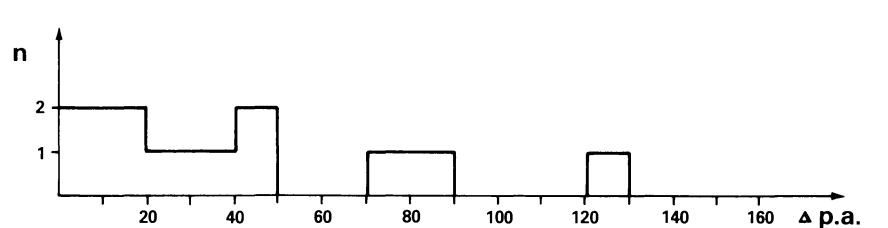


Fig. 3. Histogram of the differences in position angle (p.a.) in degrees between the milliarcsecond and arcsecond scale structures for the 11 sources where structures on both angular scales are known

deviations (Fig. 3). This contrasts with the alignment over many orders of magnitude in size shown by some powerful, extended radio galaxies. Browne et al. (1982) found a similar result in their data.

Since this paper reports only the initial results of a continuing program to monitor both the low frequency variability and the milliarcsecond structure of a number of unusually active radio sources, no discussion of models or their detailed interpretation is attempted at this stage. Fanti et al. (1983) and others have discussed the inconsistencies created by comparing size scales for low frequency variable sources derived from light travel time arguments with expected, but unobserved, high brightness temperatures ( $>10^{12}$  K).

The most attractive model at present, which can explain many of the observed properties of these very compact and active sources, such as low frequency variability and apparent "superluminal" motions, invokes synchrotron electrons and magnetic fields relativistically ejected nearly along the line of sight towards the observer (e.g. Rees, 1966, 1967; Rees and Simon, 1968). The large changes in position angles between core and arcsecond jet structures and the many "one-sided jet" morphologies found would also support such a model. However, it is interesting that 3 sources (0859 – 140, 1730 – 130, and 2251 + 158) show a "di-polar" structure about a "core," which is not as easily explained.

Acknowledgements. We are indebted to the staffs of the participating observatories for their assistance with the observing. We also acknowledge and thank the support staff of the MKII processor at the Max-Planck-Institut für Radioastronomie for their assistance with the rapid and accurate correlation of the data streams. Ms. P. Goheen and Ms. M. Dufault of the National Science Foundation have contributed greatly to the preparation of the manuscript and accompanying tables. We thank Dr. R. Fanti for critical reading of the manuscript.

The VLBI program at the Onsala Space Observatory, Chalmers University of Technology is supported by the Swedish Science Research Council; the 140' telescope at Green Bank, West Virginia is operated by the National Radio Astronomy Observatory under contract to the National Science Foundation; and the 22 m radio telescope at Crimea is supported by the Radio Astronomy Council, Soviet Academy of Sciences of the USSR.

#### References

Bååth, L.B., Rönnäng, B.O., Pauliny-Toth, I.I.K., Kellermann, K.I., Preuss, E., Witzel, A., Matveenko, L.I., Kogan, L.R., Kostenko, V.I., Moiseev, I.G., Shaffer, D.B.: 1981a, Astrophys. J. Letters 243, L123

Bååth, L.B., Elgered, G., Lundqvist, G., Graham, D., Weiler, K.W., Seielstad, G.A., Tallqvist, S., Schilizzi, R.T.: 1981b, Astron. Astrophys. 96, 316 Browne, I.W.A., Orr, M.J.L., Davis, R.J., Foley, A., Muxlow, T.W.B., Thomasson, P.: 1982, Monthly Notices Roy. Astron. Soc. 198, 673

Cocke, W.J., Pacholczyk, A.G.: 1975, Astrophys. J. 195, 279

Cohen, M.H., Moffet, A.T., Romney, J.D., Schilizzi, R.T., Shaffer,
D.B., Kellermann, K.I., Purcell, G.H., Grove, G., Swenson,
G.W. Jr., Yen, J.L., Pauliny-Toth, I.I.K., Preuss, E., Witzel, A.,
Graham, D.: 1975, Astrophys. J. 201, 249

Cohen, M.H., Unwin, S.C., Simon, R.S., Seielstad, G.A., Pearson, T.J., Linfield, R.P., Walker, R.C.: 1981, Astrophys. J. 247, 774

Cotton, W.D.: 1976a, Astrophys. J. 204, L63

Cotton, W.D.: 1976b, Astrophys. J. Suppl. 32, 467

Cornwell, T.J., Wilkinson, P.N.: 1981, Monthly Notices Roy. Astron. Soc. 196, 1967

Fanti, C., Fanti, R., Ficarra, A., Mantovani, F., Padrielli, L., Weiler, K.: 1981, Astron. Astrophys. Suppl. 45, 61

Fanti, C., Fanti, R., Ficarra, A., Gregorini, L., Mantovani, F., Padrielli, L.: 1983, Astron. Astrophys. 118, 171

Fanti, R., Ficarra, A., Mantovani, F., Padrielli, L., Weiler, K.W.: 1979, Astron. Astrophys. Suppl. 36, 359

Hunstead, R.W.: 1972, Monthly Notices Roy. Astron. Soc. 157, 367 Jones, T.W., Burbidge, G.R.: 1973, Astrophys. J. 186, 791

Kellermann, K.I., Pauliny-Toth, I.I.K.: 1968, Ann. Rev. Astron.

Astrophys. 6, 417 Ku, W.H.-M., Helfand, D.J., Lucy, L.B.: 1980, Nature 288, 323

Mantovani, F., Browne, I.W.A., Romney, J., Padrielli, L., Muxlow, T.W.B.: 1984 (in preparation)

Marscher, A.P., Broderick, J.J.: 1981, Astrophys. J. Letters 247, L49

Marscher, A.P., Broderick, J.J.: 1982, in Extragalactic Radiosources, IAU Symp. 97, eds. D.S. Heeschen, C. Wade, Reidel, Dordrecht

Matveenko, L.I., Kostenko, V.I., Papatsenko, A.Kh., Bartel, N., Massi, M., Romney, J.D., Weiler, K.W., Ficarra, A., Mantovani, F., Padrielli, L., Moiseev, I.G., Bååth, L.B., Nicolson, G.D.: 1981, Soviet Astron. Letters 7, 259

Matveenko, L.I., Kostenko, V.I., Moiseev, I.G., Romney, J.D., Bartel, N., Padrielli, L., Ficarra, A., Mantovani, F.: 1982, Soviet Astron. Letters 8, 148

McAdam, W.B.: 1976, Proc. Astron. Soc. Australia 3, 86

Miley, G.K., Perola, G.C.: 1975, Astron. Astrophys. 45, 223

Owen, F.N., Helfand, D.J., Spangler, S.R.: 1981, Astrophys. J. Letters 250, L55

Pauliny-Toth, I.I.K., Preuss, E., Witzel, A., Kellermann, K.I., Shaffer, D.B., Purcell, G.H., Grove, G.W., Jones, D.L., Cohen, M.H., Moffet, A.T., Romney, J., Schilizzi, R.T., Rinehart, R.: 1976, Nature 259, 17

Perley, R.A.: 1982, Astron. J. 87, 859

Perley, R.A., Fomalont, E.B., Johnston, K.J.: 1982, Astrophys. J. Letters 255, L93

- Phillips, R.B., Mutel, R.L.: 1982, Astrophys. J. Letters 257, L19
- Readhead, A.C.S., Wilkinson, P.N.: 1978, Astrophys. J. 223, 25
- Rees, M.J.: 1966, Nature 211, 468
- Rees, M.J.: 1967, Monthly Notices Roy. Astron. Soc. 135, 345
- Rees, M.J., Simon, M.: 1968, Astrophys. J. Letters 152, L145
- Schraml, J., Pauliny-Toth, I.I.K., Witzel, A., Kellermann, K.I.: 1981, Astrophys. J. 251, L57
- Stannard, D., Bentley, M.: 1977, Monthly Notices Roy. Astron. Soc. 180, 703
- Stannard, D., Treverton, A.M., Porcas, R.W., Davis, R.J.: 1975, Nature 255, 384
- Tananbaum, H., Wardle, J.F.C., Zamorani, G., Avni, Y.: 1983, Astrophys. J. 268, 60
- Ulvestad, J.S., Johnston, K.J., Weiler, K.W.: 1983, *Astrophys. J.* **266**, 18
- Unwin, S.C., Mutel, R.L., Phillips, R.B., Linfield, R.P.: 1982, *Astrophys. J.* **256**, 83

Soc. **190**, 269

Véron, M.P., Véron, P.: 1974, Astron. Astrophys. Suppl. 18, 309 Weiler, K.W., Johnston, K.J.: 1980, Monthly Notices Roy. Astron.